Cusp catastrophe in flow acoustics

Ingo Rehberg[a)]
Max-Planck-Institut fuer Stroemungsforschung Boettingerstr. 4-8 D-3400 Goettingen, West Germany

(Received 26 March 1984; accepted 3 July 1984)

The transonic flow in a tube following an abrupt enlargement of the cross section produces self-induced flow oscillations which generate sound (whistler). The frequency of the oscillation is influenced by the tube length: increasing length leads to a frequency decrease, but only up to a critical length l_c of the tube. If this length is further increased, the frequency will jump to higher values. This jump shows hysteresis: decreasing the tube length again leads to a jump to the lower frequency at a length $l_{c1} < l_c$. Having presented details of the above phenomenon, the two mathematical models are then presented, in which the transonic oscillator is represented by two simple nonlinear equations which behave harmonically, and the acoustic resonator, i.e., the tube, is represented by a term including a time lag. It is shown that the hysteresis vanishes for both the experiment and the model if the sound reflection at the end of the tube is decreased below a certain critical value. This behavior is one of the few reported examples of a cusp catastrophe in an oscillating system.

I. INTRODUCTION

Hysteresis phenomena in physical systems can often be interpreted as being a consequence of a subcritical bifurcation, and such bifurcations can often be shown to be part of a cusp catastrophe.[1] In fluid dynamics this has been done by Benjamin[2] and Schaeffer[3] for a steady flow. The Duffing equation, an example of a bifurcating oscillating system, has been interpreted in terms of catastrophe theory by Holmes and Rand.[4] While the Duffing equation describes a forced oscillator, the present work is concerned with a particular type of self-induced flow oscillation—the so-called base pressure oscillation. This is a special flow oscillation following a sudden enlargement of cross section in an air tube (whistler), one of the best known examples of self-induced flow oscillations accompanied by shock waves.[5,6] This flow has also been investigated theoretically by Grabitz.[7]

We concern ourselves here with the hysteretic frequency jumps of the base pressure oscillation forced by varying length l of the tube, or by varying the inlet pressure of the air flow.

II. EXPERIMENTAL RESULTS

The experimental setup is shown in Fig. 1. The nozzle is supplied with air under a maximum pressure of about 6 bar. The length l of the tube downstream of the abrupt enlargement of the cross section is continuously variable. This outer cylinder is motor driven, so that the length can slowly be changed with a speed of approximately 1 mm/sec during the experiment. The cylinder is also connected to a length transducer (Heidenhain VRZ100.070), so that the length l can be recorded by a computer (Digital PDP 11/34). The inlet pressure p_e is measured by a piezoresistive pressure transducer (Kistler 4071A10), then digitized by a voltmeter (Keithley 177DDM), and finally sent to the computer via an IEC-Bus. The sound produced by the pipe is recorded by a microphone, filtered and amplified, digitized (Digital LPA-11K), and sent to the computer memory. For the purpose of measuring sound reflection coefficients by the standing wave method, it is necessary to measure the wall pressure fluctuations within the tube. This is done using a piezoresistive Kulite XCS-093 pressure transducer. The output signal of that transducer is handled in the same way as the output of the microphone. Both the frequency and the amplitude of the sound are calculated by discrete Fourier analysis using an array processor (AP120B) connected to the PDP 11/34. A more detailed description of the computer system has been given elsewhere.[8]

The experimental parameters in this measurement are the length of the tube, the inlet pressure p_e, and the sound reflection coefficient at the open end of the outer cylinder. The values measured as a function of these parameters are the frequency and amplitude of the radiated sound. The procedure for obtaining these values is the following: 1024 samples of the output of the microphone or pressure transducer are taken by the LPA with a sampling rate of 50 kHz. Afterwards, an FFT of these 1024 measured points together with 7168 additional zeros is done by the array processor. The zeros are added to reduce the picket-fence effect below the natural uncertainty of the amplitude.

In Fig. 2 the amplitude of the oscillations measured by the microphone is plotted against the parameters pressure ratio $p = p_a/p_e$, and length l. One sees that the oscillations with a high intensity of a discrete frequency peak only occur at special values of pressure p and length l. As can be seen, the maximum amplitude is reached at $l = 50$ mm and

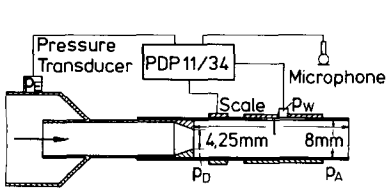

FIG. 1. Experimental setup. Either the length l of the tube or the position of the pressure transducer can be changed slowly by a motor. The sound is recorded via the pressure transducer or the microphone.

[a)] Present address: Department of Physics, University of California, Santa Barbara, California 93106.

 0031-9171/85/010090-07$01.90

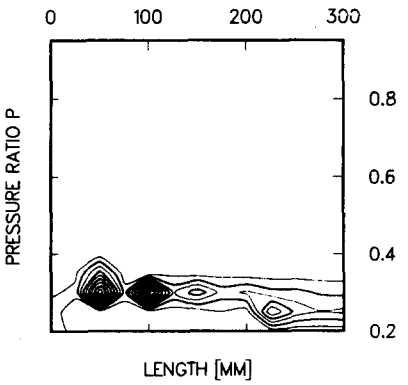

FIG. 2. Amplitude of the radiated sound versus tube length and inlet pressure.

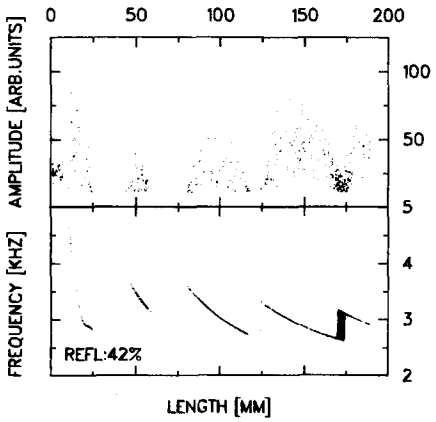

FIG. 4. Frequency and amplitude of the radiated sound as a function of tube length.

$p = 0.3$. The amplitude in both this, as well as the following measurements, is given in arbitrary units. The highest measured acoustical intensity of the sound was 115 dB(A), measured at a distance of about 1 m from the tube. Furthermore, one sees from this figure that the oscillations only take place within a certain range of pressure values. There is no shock wave in the tube for small inlet pressures, and thus no oscillations are present. The shock wave attaches to the wall for high inlet pressures, thus destroying the feedback mechanism. More details concerning the oscillation mechanism of the base pressure oscillation can be found in Refs. 5 and 7.

Figure 3 shows four typical spectra for the parameters $l = 200$ mm, $l = 220$ mm, $p = 0.25$ and $p = 0.4$. They were obtained from an FFT of 1024 samples of the output of the microphone sampled with 50 kHz. Note that almost all the power of the oscillation lies in one discrete peak and its harmonics, indicating a pure tone.

Figure 4 shows the behavior of the oscillation as a function of length for a fixed value of $p = 0.278$. The frequency of the peak with the highest intensity in the power spectrum and the intensity of that peak is plotted using a linear scale and arbitrary units. For short lengths of the tube (below 10 mm) we have a supersonic jet producing screech noise with an intensity maximum around 10 kHz, which is outside the frequency range of our plot. For $l = 10$ mm the amplitude of the highest peak in the spectrum of the radiated sound went down beyond the noise level, so that neither amplitude nor frequency values were plotted here. For lengths between $l = 10$ and $l = 25$ mm the tube produces a loud pure tone of a frequency falling from 4.8 to 2.8 kHz. There is again no measurable oscillation between $l = 25$ mm and $l = 45$ mm, followed by another range of pure tone sound ($45 \text{ mm} < l < 60$ mm) with falling frequency—and so on. One notices that the range of vanishing oscillation between $l = 120$ mm and $l = 125$ mm is fairly small and at 175 mm the oscillation does not really vanish, but rather a new phenomenon becomes apparent—the frequency jumps irregularly between the upper and the lower branch. Arrows indicate these jumps, lying so densely packed that individual arrows cannot be distinguished.

The behavior for longer tubes is shown in Fig. 5. Here the irregular frequency jumps between the two states has vanished and one observes a true hysteretic behavior instead, for instance, at $l = 280$ mm. By this we mean that if the tube oscillates with the higher frequency, it will remain on that branch; if one then decreases the length below 270 mm and increases it to 280 mm again, the flow will oscillate with the lower frequency, this latter being also a stable state. Notice that the hysteresis domain increases with the length of the tube: it is small at $l = 160$ mm, larger at $l = 220$ mm, and largest at $l = 280$ mm. One difference between the measure-

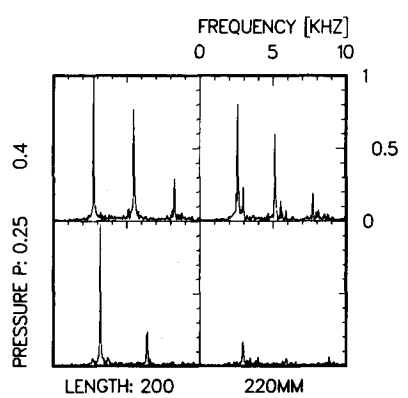

FIG. 3. Four typical spectra.

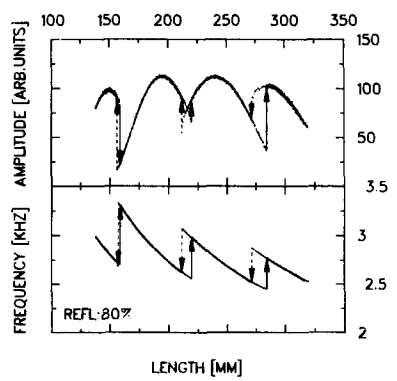

FIG. 5. Frequency and amplitude of the pressure measured inside the tube as a function of tube length.

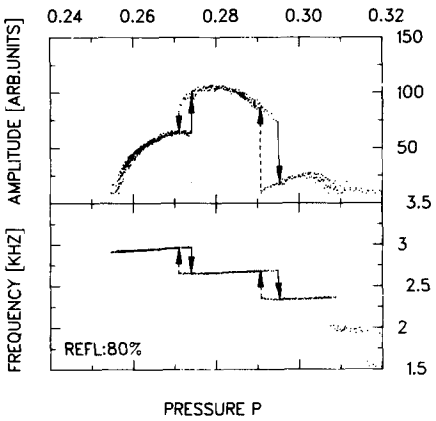

FIG. 6. Frequency and amplitude of the pressure measured inside the tube as a function of inlet pressure.

ments in Figs. 4 and 5 is that a diffusor was connected to the tube end, thereby increasing the sound reflection coefficient and the hysteresis domains. A further difference is that pressure measurements for the latter were made by the pressure transducer within the tube and not by the microphone outside the tube. Therefore, the amplitude behavior is much more regular than that of Fig. 4. The pressure was measured at a distance of 105 mm from the end of the tube.

What happens if the length l of the tube is held constant and only the pressure p is changed? The answer is shown in Fig. 6. Both the frequency and the amplitude of the pressure measured inside the tube used for the last figure are plotted against the pressure ratio p, p having first been decreased and then again increased. Note the hysteretic jumps at $p = 0.27$ and $p = 0.3$.

A further question is whether these hysteretic frequency jumps are characteristic for the base pressure oscillation. To shed some light on this problem, the sound reflection coefficient of the end of the cylinder was decreased. This was done by drilling holes and longitudinal slits into the cylinder beginning at a distance of approximately 100 mm from the end of the tube. The result is shown in Fig. 7. The amplitude of the oscillation when compared to that of Fig. 6 is reduced and the frequency is now a smooth function of the pressure—without any jumps at all. There seems to be an optimal pressure ratio for the base pressure oscillation where its amplitude has a maximum. The frequency of the oscillation increases with decreasing pressure ratio.

This last experiment suggests that something may be gained by measuring the sound reflection coefficient. This was done using the standing wave method. Figure 8 shows two examples. While the base pressure oscillation was maintained by a fixed pressure p, the pressure transducer was moved over a slit of 1 mm thickness along the tube length. The procedure for getting the amplitude of the oscillation is the same as described above. The points show measured amplitudes, and the solid line is a least squares fit to the function

$$A(x) = [f1 + f2^* \sin(f3^* x + f4)]^{0.5}, \tag{1}$$

where A is the amplitude, x is the position of the transducer, and $f1$–$f4$ are the fitting parameters. The reflection coefficient is thus

$$r = \frac{(f1+f2)^{0.5} - (f1-f2)^{0.5}}{(f1+f2)^{0.5} + (f1-f2)^{0.5}}. \tag{2}$$

Having shown experimental curves both with and without hysteretic frequency jumps, we can formulate perhaps the most interesting question of this paper: If there are jumps for high sound reflection coefficients and no jumps for low sound reflection coefficients, what is the behavior between these two extremes? The experimental answer is given in Fig. 9. Here the frequency as a function of the resonator length is shown for four different sound reflection coefficients of the tube. To obtain the different sound reflection coefficients, we sawed a cross slit 120 mm from the end of the tube with the low sound reflection coefficient. The area of the above slit could be varied by means of a ring. If open, the sound reflection coefficient is about 0.4; when closed, however, it is less than 0.1. The lowest frequency curve of Fig. 9 shows the result for the closed slit. The frequency seems to be a smooth function of l. Near $l = 275$ mm there is some sort of critical behavior, though the frequency of the oscillation is not well defined here. This effect is clearly visible for $r = 0.17$, but still weaker for $r = 0.26$. For $r = 0.37$ the frequency jumps irregularly between two discrete values. The explanation for this behavior will be given in Sec. IV.

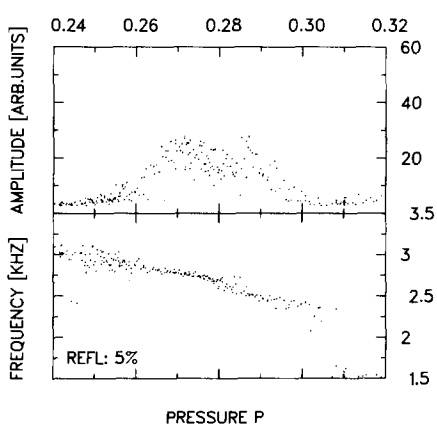

FIG. 7. Frequency and amplitude of the wall pressure measured within the tube as a function of inlet pressure for a small sound reflection coefficient.

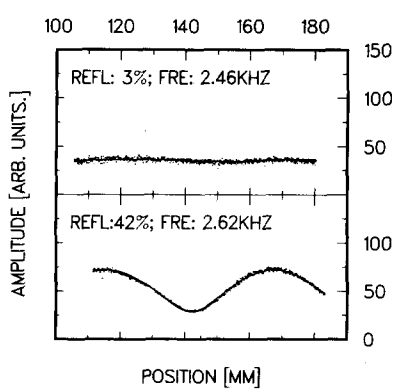

FIG. 8. Two examples of standing wave measurements for the determination of the sound reflection coefficient.

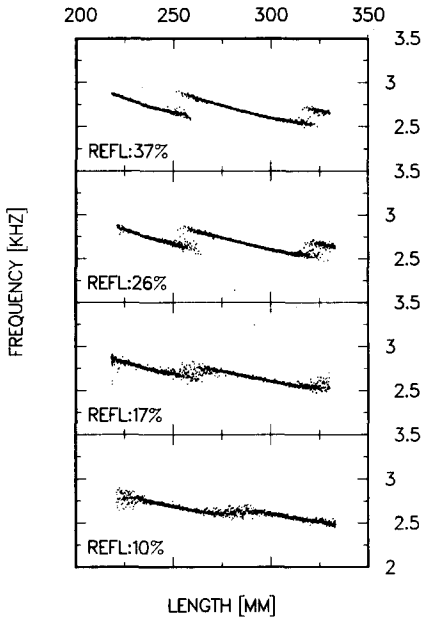

FIG. 9. Frequency of the wall pressure measured within the tube as a function of length for four different sound reflection coefficients.

III. TWO QUALITATIVE MODELS

The behavior described in the last section, i.e., hysteretic frequency changes caused by the variation of the length of an acoustical resonator, not only occurs in our special kind of flow oscillation, but has also been observed for a reed pipe by Vogel.[9] This led to the idea that for a mathematical simulation the oscillator could simply be globally accounted for. To this end, we numerically studied the interaction of the resonator with (i) the well-known van der Pol oscillator and (ii) another self-induced oscillator.

To understand the motivation for using the following equations, one must first consider the mechanics of the air flow oscillation. Here we follow Grabitz.[7] The pressure p_d in the dead-air region determines the exit angle of the supersonic jet, the position of the shock wave, and the pressure downstream of the shock. This pressure can in turn effect the dead-air pressure p_d via that thin volume near the wall where no shock wave is present. This system thus forms a feedback loop which may give rise to self-induced oscillations. On the basis of these thoughts, Grabitz established a simplified numerical model for the flow, and the numerical evaluation of his system of differential equations led to the correct values of the oscillation frequency. For the purpose of this work two points are relevant: the pressure feedback loop and the nonlinear terms in the feedback to prevent the amplitude of the oscillation from growing beyond all bounds. One of the most simple differential equations with these properties is the van der Pol equation

$$A(t)'' + m[A(t)^2 - 1]A(t)' + A(t) = 0, \qquad (3)$$

which was originally constructed for the description of self-induced electrical oscillations.

How would one approach modelling the resonator? If the dead air pressure p^d changes, this leads to a change of the pressure downstream of the shock. This propagates through

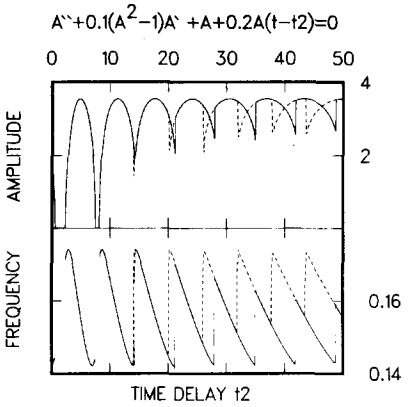

FIG. 10. Interaction of the van der Pol equation with a time-lag term.

the tube as an acoustic wave, is reflected to a certain extent at the end of the tube, and propagates back into the dead air region, thus interacting with its source after some time delay given by the speed of sound and the length of the tube. We thus studied the equation

$$A(t)'' + m[A(t^2) - 1]A(t)' + A(t) + cA(t - t2) = 0. \qquad (4)$$

The first three terms represent the self-induced oscillator; the additional term with the deviating argument represents the influence of the resonator. Here c is a measure of the sound reflection coefficient, and $t2$ is the total time for a pressure fluctuation to propagate through the tube.

Figure 10 shows some results for the above equation obtained thus: beginning with a time lag $t2 = 0$ and starting with random numbers, Eq. (4) was integrated numerically by a standard Runge–Kutta method. When the system reached an equilibrium position, the frequency and the amplitude of the state were stored. Here $t2$ was then increased, and, starting with the old values of $A(t)$, iterated until a new steady state was reached. This process was repeated until $t2$ reached the value of 40, after which all values of the frequency and amplitude had been connected by the solid line. The procedure then was repeated, but now with decreasing $t2$ (dashed

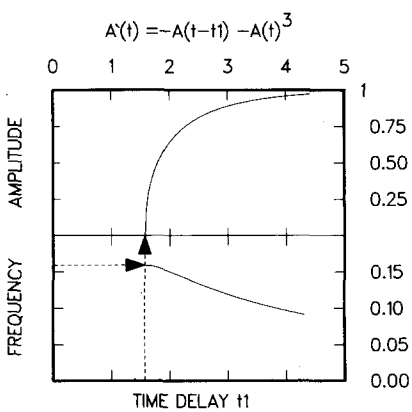

FIG. 11. Supercritical bifurcation for a nonlinear equation with a deviating argument. The dashed arrows point to the values obtained by a linear stability analysis.

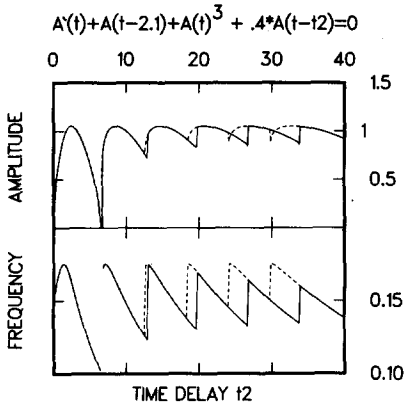

FIG. 12. Interaction of nonlocal equation with a time-lag term.

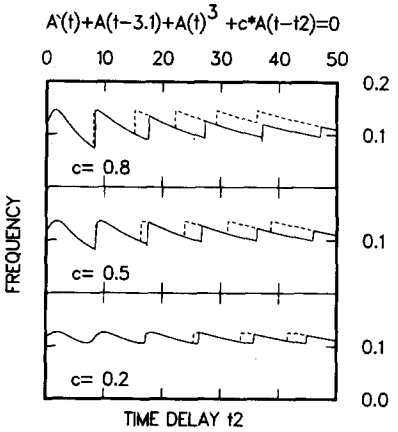

FIG. 13. Frequency as a function of delay time for three different values of c representing sound reflection coefficients.

line). If we compare this figure with the measurements in Figs. 4 and 5, there are two qualitative agreements: (i) For certain small resonator lengths (small values of $t\,2$) the amplitude goes to zero. (ii) Hysteretic frequency jumps may occur for larger resonator lengths (large values of $t\,2$), and the thickness of the hysteresis region increases with increasing resonator length.

One may argue that the van der Pol oscillator equation is very special, and the agreement between physical and numerical experiment is therefore not very convincing. We thus also studied the time-lag term representing the acoustical resonator with another kind of differential equation leading to self-induced oscillations. This time we took the oscillator equation

$$A'(t) + A(t - t\,1) + A(t)^3 = 0. \tag{5}$$

Because this kind of oscillator equation is not so well known as the van der Pol equation, Fig. 11 may help to acquaint one with it. Here the amplitude and frequency of the oscillation is plotted against $t\,1$. Note that there is no oscillation for $t\,1$ less than $\pi/2$, where the system undergoes a Hopf bifurcation. Both the critical point $\pi/2$ as well as the frequency $1/(2\pi)$ at that point can be easily obtained by a linear analysis.[8] The dashed arrows point to these values, thus giving some indication of the quality of the numerical procedure. Above the critical value, the system oscillates with a well-defined amplitude and frequency. It is possible that there are also more complicated "chaotic" solutions for higher values of $t\,1$, but for the values we used, no behavior of that kind was observed.

In Fig. 12, $t\,1$ was chosen as 2.1, and this oscillator equation was combined with a time-lag term representing the resonator. This led to

$$A'(t) + A(t - 2.1) + A(t)^3 + cA(t - t\,2) = 0. \tag{6}$$

The procedure for obtaining both the solid and the dashed line has been the same as described in connection with Eq. (4), and the results are qualitatively the same (see Fig. 10).

IV. CUSP CATASTROPHE

Having established a sufficient model for describing the hysteretic frequency changes, an important question remains: for high sound reflection coefficients, there are hysteretic jumps, and, for a reflection coefficient of zero, there is clearly no influence on the oscillation at all. Thus on decreasing the reflection coefficient, there must be a critical point where the hysteretic jumps cease. What is happening in the neighborhood of this critical point—in particular: how does the frequency behave and how does the hysteresis domain vanish?

An answer to the first question is given in Fig. 13. For high sound reflection coefficients ($c = 0.8$, lower curve) there is a clearly visible frequency jump between $t\,2 = 5$ and $t\,2 = 10$; for $c = 0.5$ the range of hysteresis becomes smaller and for $c = 0.2$ the frequency is a smooth function of $t\,2$, hysteresis having vanished. The critical point is accompanied by an infinite slope of the frequency curve.

Figure 14 shows the bifurcation set[1] for the model (4) as obtained from the numerical experiment. The points show jumps from the higher to the lower frequency, the crosses, jumps from lower to higher frequency. The solid line is a least squares fit to a linear deformation of a semicubic parabola. This fit is justified in the neighborhood of the critical point: catastrophe theory[1] tells us that there should be a diffeomorphism mapping a semicubic parabola into the bifurcation set, and near the critical point we can truncate the diffeomorphism to a linear mapping. There is a visible devi-

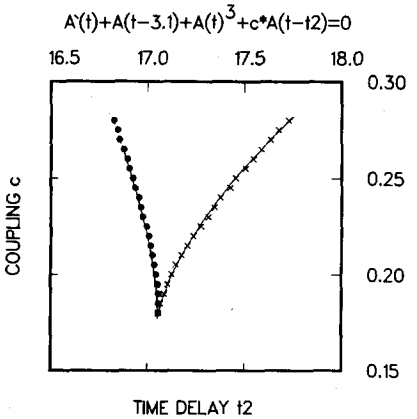

FIG. 14. Bifurcation set for the model equation.

ation near the critical point of the fitted curve from the numerical experiment. This is probably because the system is very sensitive to perturbations near the critical point, the necessarily unsteady change of time-lag t 2 being such a disturbance.

Catastrophe theory, a theory dealing with singularities of smooth mappings or gradient dynamical systems, is not necessarily applicable here. It is the underlying assumption that the frequency is a smooth folded function of the parameters as illustrated in Fig. 15. Here the way in which the hysteresis domain vanishes is shown by plotting the frequency as a function of the resonator length and the sound reflection coefficient. The dashed line in the center has an infinite slope everywhere, the other dashed lines being its projections. Notice that, despite the fact that the line itself is smooth, the projection onto the length/reflection plane is cusped. It is this feature which led to the name cusp catastrophe. For other illustrations of such surfaces, refer to Ref. 1. There are three possible frequencies for any single pair of values of length t 2 and reflection coefficient c lying within the cusped region. The numerical experiment reached only the upper- or lower-frequency branch—the unstable solution separating the two stable solutions has not been proved to exist for our special kind of nonlinear equation.

In Fig. 15 one sees that small changes of the experimental parameters cause large changes of the frequency near the critical point. This sensitivity to disturbances has also been observed in the numerical experiment (Fig. 14), but is much more important for the physical experiment. The disturbances in the tube result from the turbulent character of the flow. This explains the irregular frequency jumps near the critical point as shown in Fig. 9. Here the frequency is not well defined, but jumps within a relatively broad range of values.

From Fig. 9 it should have become clear that it is not possible to measure the bifurcation set (similar to Fig. 14) in the physical experiment near the critical point because of the large fluctuations caused by turbulence. Instead, we have used a least squares fit to a cubic polynomial in order to determine the critical point in the experiment. The result is shown in Fig. 16. Notice that the frequency is not a unique function of the length, but that in a neighborhood of the

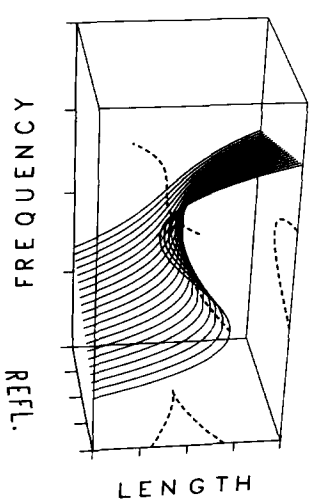

FIG. 15. Three-dimensional qualitative explanation for the frequency jumps. The central dashed line has an infinite slope, the other three are projections.

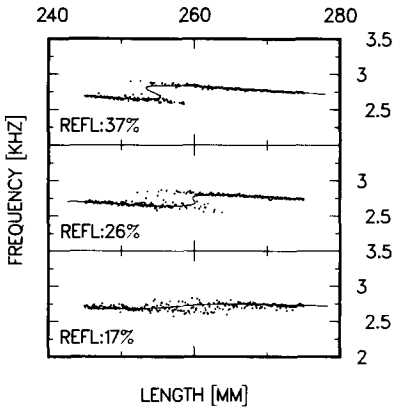

FIG. 16. Measured frequency as a function of length, together with a local fit to a cubic polynomial.

critical point the length is a unique function of the frequency. For this reason the fitting procedure was done using the latter function. The underlying philosophy for using such a fit is that near the critical point the curve may fluctuate from a subcritical shape without bistability to a supercritical shape with bistability. The small number of frequency values lying between the two branches is probably because turbulence briefly makes the curve subcritical. In that sense the function is fitted to a time-averaged curve. The fluctuations destroy the sharp distinction between subcritical and supercritical behavior—a fact that is also well known in other hydrodynamic instabilities.

In Fig. 16 the curve fitted to the experimental data for a reflection coefficient of 17% is subcritical. The discriminant of the cubic is positive. For 26% the discriminant is negative, indicating a supercritical behavior. The critical point is defined by a vanishing discriminant. Linear interpolation between the two curves leads to a critical value of 26%.

V. CONCLUSION

We have shown that an acoustical resonator of the kind used in the experiment can be described by a time-lag term. This is of some interest because such equations, although complicated from a mathematical point of view, are simple to handle with digital computers.

We have shown further that both the hysteretic frequency jumps of the base pressure oscillations as well as those in the mathematical models can be understood as being part of a cusp catastrophe. This explanation leads to a qualitative understanding of the phenomena observed near the critical point.

ACKNOWLEDGMENTS

I would like to thank Professor E.-A. Müller for giving me the opportunity to do this work at the Max-Planck Institute of Fluid Dynamics. I am grateful to Professor E. O. Schulz-DuBois and Dr. G. E. A. Meier for many valuable hints. I had the pleasure of discussing many of the difficulties with my colleagues Dipl. Phys. R. Timm and Dipl. Phys. D. Auerbach.

This work was supported in part by the Deutsche Forschungsgemeinschaft.

[1]T. Poston and I. Stewart, *Catastrophe Theory and Its Applications* (Pitman, London, 1978).
[2]T. B. Benjamin and T. Mullin, J. Fluid Mech. **121**, 219 (1982).
[3]D. G. Schaeffer, Math. Proc. Cambridge Philos. Soc. **87**, 307 (1980).
[4]P. J. Holmes and D. A. Rand, J. Sound Vib. **44**, 247 (1976).
[5]J. S. Anderson, W. M. Jungowski, W. J. Hiller, and G. E. A. Meier, J. Fluid Mech. **79**, 769 (1977).
[6]J. S. Anderson and G. E. A. Meier, Rep. Max-Planck-Institut Stroemungsforsch. 1 (1982).
[7]G. Grabitz, Z. Angew. Math. Mech. **58**, T 273 (1978).
[8]I. Rehberg, Mitt. Max-Planck-Institut Stroemungsforsc. 75 (1983).
[9]H. Vogel and M. Wien, Ann. Phys. **62**, 649 (1920).